Combined heat and power dynamic economic dispatch considering field operational characteristics of natural gas combined cycle plants

Haiquan Yu[1, 2], Jianxin Zhou[1, *], Fengqi Si[1], Lars O. Nord[2]

[1] Key Laboratory of Energy Thermal Conversion and Control of Ministry of Education, School of Energy and Environment, Southeast University, Nanjing, 210096, P.R. China

[2] Department of Energy and Process Engineering, Norwegian University of Science and Technology - NTNU, Trondheim, Norway

Corresponding author: Jianxin Zhou

E-mail addresses: zjx@seu.edu.cn (Jianxin Zhou), yhq@seu.edu.cn (Haiquan Yu), fqsi@seu.edu.cn (Fengqi Si), lars.nord@ntnu.no (Lars O. Nord)

Address: School of Energy & Environment, Southeast University, No.2 Sipailou Road, Nanjing, 210096, China.

Tel: +86 25 83793454.

ABSTRACT

Combined heat and power dynamic economic dispatch (CHPDED) is one of the key technologies for the efficient operation of natural gas combined cycle (NGCC) plants in integrated energy systems. In this study, based on the actual operational characteristics of NGCC plants at combined heat and power mode, a plant advanced loads variation capacity model is developed. The advanced loads variation capacity models of NGCC plants are integrated into the CHPDED model to guarantee the feasibility of the dispatched demands. Moreover, a field operational data based simplification method for the advanced loads variation capacity model is proposed to alleviate the computational burden. The field operational data of an actual NGCC station is taken to perform case studies. The calculation cases show that all the dispatched demands calculated from the CHPDED model with advanced loads variation capacity models are feasible. Furthermore, the influence of the heat load variation process on the power load adjustment process is employed to achieve better dispatch results. Compared with CHPDED models in the existing research, the CHPDED model with advanced loads variation capacity models significantly improves the feasibility of the dispatched demands, thereby enhancing the real application value of CHPDED in the field operation of NGCC plants.

Keywords: Combined heat and power (CHP); Economic dispatch (ED); Feasibility; Natural gas combined cycle (NGCC); Combined cycle gas turbine (CCGT)

1 Introduction

1.1 Background

Due to the growing prominence of the energy crisis and environmental pollution, the development of more efficient energy consumption and management patterns has been promoted [1,2]. In recent years, integrated energy systems have attracted extensive attention [3-5], in which various energy sectors are integrated to realize energy complementation and cascade utilization. In multiple types of integrated energy systems, combined heat and power (CHP) plants are taken as the core and basic energy conversion sector to satisfy various demands [5,6]. Among the heavy-duty industrial CHP plants, natural gas combined cycle (NGCC) plants at CHP mode have the excellent performance on efficiency and operational flexibility [7-9]. As one of the major tasks for the operators of a power station in integrated energy systems, combined heat and power dynamic economic dispatch (CHPDED) aims to arrange and schedule the demands of each plant for achieving the best system performance [10-12].

The research on dealing with the CHPDED problem has appealed to many scholars, of which the research targets were mainly focused on the following directions: (1) higher operational flexibility, (2) better robustness, (3) less emission, and (4) less computational burden. (1) Some research aimed to improve the system operational flexibility with the utilization of auxiliary facilities or heat storage of the district heating (DH) system. In the research [13], a novel CHPDED framework was presented for the CHP plants with heat storage facilities. A coordination control system and a plant-level energy management system were integrated into the dispatch model to fully employ the adjustment capacity of the heat storage facilities. In the work [14], heat storage facilities and electric boilers were utilized

to decouple the strong interdependence between power generation and heat generation of CHP plants at the heat-led mode. The CHPDED calculation proved that the power demand fluctuation resulted from the intermittent renewable energy could be partly stabilized by the heat storage facilities. Deng et al. [15] attempted to decouple the strong interdependence between power generation and heat generation of CHP plants with the help of heat pumps. A real-code quantum optimization-based bi-level programming model was developed to dispatch power and heat demands at different levels. Yu et al. [16] carried out an analysis and comparison on the influence of electric boilers and heat pumps on the system performance under the framework of CHPDED. A simplified equivalent thermal characteristic model of the DH network and buildings was formulated to take their thermal inertial into consideration. In the work [17], a hierarchical CHPDED scheme was designed to utilize the power adjustment flexibility provided from the DH system, based on the proposed flexibility indicators for an integrated energy system. Li et al. [23] developed a CHPDED model for the integrated energy system containing advanced adiabatic compressed air energy storage, of which the off-design performance was taken into account.

(2) Some scholars tried to take the uncertainties of various operating conditions into account, thereby developing the CHPDED model with robustness. In the research [18,24], a two-stage robust CHPDED model was presented to deal with the uncertainties of wind power, ambient temperature, and heat dissipation of heating pipelines in DH network. The worst uncertainty scenarios of wind power and heat demands were considered at the second stage. Turk et al. [19] developed a two-stage stochastic CHP scheduling scheme to take full advantage of the power generation reserve for offsetting the wind power uncertainty. Li et al. [31] developed a probability-interval-based CHPDED model, in which the electricity storage facilities were introduced to counteract the influence of wind power uncertainty. In the work [32], an adaptive robust CHPDED model considering the uncertainties of power demands and outdoor temperature was presented, for the sake of system operational reliability and end-users' thermal comfort. (3) Emission problem was considered into the CHPDED calculation in some research. Eladl et al. [20] carried out a multi-objective CHPDED model for the maximum economic benefit and minimum CO2 emission, with the consideration on uncertainties of wind and photovoltaic power, and multi-type energy storage devices. In the work [25], ladder carbon trading mechanism was integrated into the cost function of the CHPDED model for an electricity-thermal-natural gas coupling system. Mohammadi et al. [33] presented an environmental CHPDED model considering the detailed thermal characteristic of heat storage facilities, and compared the calculation results under different operation strategies and components configurations. (4) There were also some studies focused on improving the calculation method of the CHPDED model for alleviating the computational burden. Yi et al. [21] developed a distributed neurodynamic based optimization method for CHPDED calculation, in which the parallel computation framework was adopted to accelerate convergence. In the research [34], an innovative multi-objective optimization framework that integrated the ε-constraints method and Hammersley sequence sampling method was presented.

However, the improvements on CHPDED models in the above research were mainly focused on the objective function, while the feasibility of the dispatched demands of CHP plants has not been paid sufficient attention. The CHPDED models in the above research were generally developed on the basis of some assumptions and simplifications of the operational characteristics of CHP plants, but part of these treatments are not applicable to NGCC plants at CHP mode. As a result, the feasibility of the

dispatched demands is influenced greatly as shown in the calculation cases in this study. In terms of static thermal characteristics, to the best of the authors' knowledge, in most reported works [23-30] the ambient temperature is not considered into the plant characteristic when carrying out CHPDED calculation for NGCC plants. But the performance of an NGCC plant is affected by the ambient temperature considerably, such as the feasible operating zone (FOZ) and the fuel consumption characteristic. With the variation of ambient temperature, the boundary of the FOZ and the loads adjustment range of an NGCC plant change obviously. For the reference 1×1 NGCC plant in this study, the difference in fuel consumption at 100% gas turbine load fraction reaches up to about 16% under various ambient temperature. In terms of dynamic thermal characteristics, the loads variation capacity of a CHP plant, represented by the load ramp rates in some research, is set to constants in most CHPDED models [13-30]. There are even CHPDED models that do not constrain the loads variation capacity of plants in the literature [31-37]. At present most CHP plants are operated at heat-led mode [17,29,38-41], which means the reliability of the heat generation process has priority over the power generation process. The plant power load adjustment process and capacity are significantly impacted by the heat load variation process. In addition, there are several turbines in an NGCC plant, with the result that the loads variation characteristics are more complicated and should not be set to constants. Therefore, as the complex operational characteristics of NGCC plants at CHP mode are not considered adequately in the CHPDED models in most literature, part of the dispatched demands will be unfeasible in the actual operation of plants. If the NGCC plants run according to the existing CHPDED models, the balance between generation and demands may be broken. This negatively influences the operational reliability and security of the NGCC station and the integrated energy system.

1.2 Research challenge and contribution

Operational reliability and security are the most fundamental requirements for the power plants and stations. Due to the rough formulation of the operational characteristics of NGCC plants, the calculation results of CHPDED models in the existing research may be unfeasible. In order to fill the research gap, this study aims to propose a reliable and applicable CHPDED model for NGCC plants, in which the actual operational characteristics of NGCC plants are taken into consideration in detail. In this study, an advanced loads variation capacity (LVC) model of NGCC plants at CHP mode is developed, and further integrated into the CHPDED model for improving the feasibility of dispatched demands. Moreover, in order to avoid increasing the computational burden of the CHPDED model, a field operational data based simplification method for the advanced LVC model is proposed. Finally, CHPDED calculation on several demand scenarios of an actual NGCC station is performed as case studies, which include the demand scenarios of four typical days and three assumed future demand scenarios. The calculation results prove the applicability and necessity of the CHPDED model with advanced LVC models. The main contributions of this study are as follows:

(1) Based on the actual operational characteristics of an NGCC plant at CHP mode, a plant advanced LVC model is developed. The relative feasible operating zone is proposed to depict the heat and power loads variation capacity of the plant. Parameters of the model are assigned with the field operational data to accurately represent the actual loads variation capacity of NGCC plants.

(2) A CHPDED model applicable for NGCC plants is presented. The advanced LVC models of

NGCC plants are integrated into the CHPDED model to guarantee the feasibility of dispatched demands. Furthermore, based on the field operational data, the advanced LVC model is simplified properly to alleviate the computational burden of the CHPDED model.

(3) Compared with CHPDED models in the existing research, the CHPDED model with advanced LVC models significantly improves the feasibility of the dispatched demands. On the premise of guaranteeing operational reliability, the CHPDED model with advanced LVC models can promote the economic performance of the NGCC station. The real application value of CHPDED in the field operation of the NGCC station is enhanced.

The remainder of this paper is organized as follows. In Section 2 the plant advanced LVC model and the field operational data based simplification method are elaborated. In Section 3 the plant parameters in the CHPDED model are assigned based on the field operational data of an actual NGCC station. In Section 4 the calculation results of the CHPDED models with general LVC models and advanced LVC models are showed and analyzed. Section 5 presents the conclusion.

2 Methodology

2.1 CHPDED model

An NGCC plant is mainly comprised of gas turbine, heat recovery steam generator (HRSG), steam turbine and auxiliary facilities. Generally, every gas turbine is equipped with a HRSG, in which the feedwater is heated into live steam with different pressures. Then the live steam is led into the steam turbine. When the plant is operated at CHP mode, the process steam is extracted from the steam turbine. For an NGCC station with several plants, the CHPDED problem is to economically arrange the power and heat demands of each plant at each dispatch time interval. It aims to achieve the minimum total fuel consumption over the operating horizon on the premise of meeting various constraints. For the CHPDED model with N plants and T dispatch time intervals, the objective function can be formulated as:

$$\text{Minimize} \sum_{t=1}^{T}\sum_{i=1}^{N} C_i\left(P_{\mathrm{D},i}(t), Q_{\mathrm{D},i}(t), T_{\mathrm{A}}(t)\right)\cdot\Delta t \tag{1}$$

where C_i is the fuel consumption function of the ith (i = 1, 2, …, N) NGCC plant. $P_{\mathrm{D},i}(t)$ and $Q_{\mathrm{D},i}(t)$ are the dispatched power and heat demands of the ith plant at the tth (t = 1, 2, …, T) dispatch time interval, respectively. $T_{\mathrm{A}}(t)$ is the ambient temperature at the tth dispatch time interval. Δt is the span of a dispatch time interval.

The minimization task of the CHPDED problem should be subjected to the following demands balance and plants operating constraints:

(1) System generation and demands balance constraints

At each dispatch time interval, the total power generation of plants should be balanced with the demand from the power grid. The total heat generation of plants should also be balanced with the demand from the DH system.

$$\sum_{i=1}^{N} P_{\mathrm{D},i}(t) = P_{\mathrm{PG}}(t), \quad \forall t \in [1,2,\cdots,T] \tag{2}$$

$$\sum_{i=1}^{N} Q_{\mathrm{D},i}(t) = Q_{\mathrm{DH}}(t), \quad \forall t \in [1,2,\cdots,T] \tag{3}$$

where $P_{\mathrm{PG}}(t)$ is the power demand from the power grid at the tth dispatch time interval. $Q_{\mathrm{DH}}(t)$ is the heat demand from the DH system at the tth dispatch time interval.

(2) Plant generation capacity constraints

The power and heat generation capacity of a CHP plant are interdependent and can be represented by the FOZ. For an NGCC plant, the FOZ is influenced by the ambient temperature.

$$P_i^{\min}\left(Q_{\mathrm{D},i}(t), T_{\mathrm{A}}(t)\right) \le P_{\mathrm{D},i}(t) \le P_i^{\max}\left(Q_{\mathrm{D},i}(t), T_{\mathrm{A}}(t)\right), \quad \forall i \in [1,2,\cdots,N],\ \forall t \in [1,2,\cdots,T] \tag{4}$$

$$Q_i^{\min}\left(P_{\mathrm{D},i}(t), T_{\mathrm{A}}(t)\right) \le Q_{\mathrm{D},i}(t) \le Q_i^{\max}\left(P_{\mathrm{D},i}(t), T_{\mathrm{A}}(t)\right), \quad \forall i \in [1,2,\cdots,N],\ \forall t \in [1,2,\cdots,T] \tag{5}$$

where $P_i^{\min}$ and $P_i^{\max}$ are the minimum and maximum power generation capacity functions of the ith NGCC plant. $Q_i^{\min}$ and $Q_i^{\max}$ are the minimum and maximum heat generation capacity functions of the ith NGCC plant.

(3) Plant loads variation capacity constraints

The loads variation capacity of a plant is defined as the range that the power and heat loads can change within a period of time. For the sake of operational reliability and security, the required loads variation of a plant between two adjacent dispatch time intervals should be limited by its loads variation capacity.

$$\Delta P_{\mathrm{C},i}^{\min} \le P_{\mathrm{D},i}(t) - P_{\mathrm{D},i}(t-1) \le \Delta P_{\mathrm{C},i}^{\max}, \quad \forall i \in [1,2,\cdots,N],\ \forall t \in [1,2,\cdots,T] \tag{6}$$

$$\Delta Q_{\mathrm{C},i}^{\min} \le Q_{\mathrm{D},i}(t) - Q_{\mathrm{D},i}(t-1) \le \Delta Q_{\mathrm{C},i}^{\max}, \quad \forall i \in [1,2,\cdots,N],\ \forall t \in [1,2,\cdots,T] \tag{7}$$

where $\Delta P_{\mathrm{C},i}^{\min}$ and $\Delta P_{\mathrm{C},i}^{\max}$ are the minimum and maximum power load variation capacity of the ith NGCC plant. $\Delta Q_{\mathrm{C},i}^{\min}$ and $\Delta Q_{\mathrm{C},i}^{\max}$ are the minimum and maximum heat load variation capacity of the ith NGCC plant. The calculation method of these four parameters of an NGCC plant is elaborated in the next section.

2.2 Advanced LVC model of NGCC plants

In this section, the general LVC model and the advanced LVC model of an NGCC plant at CHP mode are elaborated. In the literature [13-30], the heat and power loads ramp rates of a CHP plant are set to constants, resulting in the loads variation capacity being also constants in the CHPDED model. In the literature [23-30] the power load ramp rate of an NGCC plant is represented by the output variation rate of gas turbine, without taking the output variation rate of steam turbine into account. In this work, the loads variation capacity formulations of an NGCC plant utilized in the above literature are called “general LVC model”. In the general LVC model, the heat load variation capacity (ΔQ_{C}, MW) and power load variation capacity (ΔP_{C}, MW) within Δt time can be written as:

$$\Delta Q_{\mathrm{C}} = \int_{t_0}^{t_0+\Delta t} \left(\pm R_{\mathrm{H}}\right) dt \tag{8}$$

$$\Delta Q_{\mathrm{C}}^{\max} = R_{\mathrm{H}} \Delta t \tag{9}$$

$$\Delta Q_{\mathrm{C}}^{\min} = -R_{\mathrm{H}}\Delta t \tag{10}$$

$$\Delta P_{\mathrm{C}} = \int_{t_0}^{t_0+\Delta t} \left(\pm R_{\mathrm{GT}}\right) dt \tag{11}$$

$$\Delta P_{\mathrm{C}}^{\max} = R_{\mathrm{GT}}\Delta t \tag{12}$$

$$\Delta P_{\mathrm{C}}^{\min} = -R_{\mathrm{GT}}\Delta t \tag{13}$$

where R_{H} is the plant heat load ramp rate (MW/min), and R_{GT} is the output variation rate of gas turbine (MW/min). t_0 is the starting time of a dispatch time interval in the CHPDED model.

It should be noted that in most of the above literature, the span of a dispatch time interval in the CHPDED problem is 1 hour. Due to the large output variation rate of gas turbine, it is enough for an NGCC plant to adjust from the minimum operating load to the nominal load in 1 hour. Thus, it is acceptable that the plant power load ramp rate is set to a constant, or even not limited. However, with the development of the demands forecast technology, the resolution of the day-ahead demands forecast currently used in the field operation has been 5 minutes. In this situation, the plant power load ramp rate should not be set to a constant. It is necessary to develop a more accurate LVC model for NGCC plants at CHP mode based on the field operational characteristics, i.e. “advanced LVC model” in this work.

At present most CHP plants are operated at heat-led mode [17,29,38-41], which means the reliability of the heat generation process has priority over the power generation process. Therefore, the heat load variation capacity of a CHP plant is mainly dependent on the heat load ramp rate, while the power load variation process and capacity are influenced by the heat load variation process. The heat load variation capacity (ΔQ_{C}) in the advanced LVC model is the same as that in the general LVC model, as shown in Eq. (8) ~ (10). The power load variation capacity (ΔP_{C}) of an NGCC plant is determined by the outputs of gas turbine and steam turbine, and can be written as:

$$\Delta P_{\mathrm{C}} = \int_{t_0}^{t_0+\Delta t} \left(\alpha R_{\mathrm{GT}} + R_{\mathrm{ST}}\right) dt \tag{14}$$

where R_{ST} is the output variation rate of steam turbine (MW/min), of which the calculation method is elaborated below. α represents the output variation direction of gas turbine, which equals 1 when the gas turbine output rises, and −1 when the gas turbine output falls.

In an NGCC plant the steam turbine output (P_{ST}) is mainly determined by the live steam parameters of each water-steam circuit and the heat load (Q). The live steam parameters are mainly determined by the temperature and mass flow of gas turbine exhaust gas, which are the function of gas turbine output (P_{GT}) and ambient temperature (T_{A}). The above relationship can be organized as:

$$P_{\mathrm{ST}} = f\left(P_{\mathrm{GT}}, T_{\mathrm{A}}, Q\right) \tag{15}$$

As a result, at given ambient temperature, the changes of gas turbine output and heat load jointly determine the output variation rate of steam turbine (R_{ST}), which can be calculated as:

$$R_{\mathrm{ST}}\left(t\right) = \beta R_{\mathrm{ST}}^{\mathrm{H}}\left(t\right) + R_{\mathrm{ST}}^{\mathrm{GT}}\left(t\right) \tag{16}$$

where $R_{\mathrm{ST}}^{\mathrm{H}}(t)$ and $R_{\mathrm{ST}}^{\mathrm{GT}}(t)$ are the output variation rates of steam turbine caused by the heat load change

and the gas turbine output change at the time of t, respectively. β represents the output variation direction of steam turbine caused by the heat load change. The heat load and steam turbine output are negatively correlated. When the flow of extracted process steam increases, the heat load will rise and steam turbine output will fall, and β equals −1. When the flow of extracted process steam decreases, the heat load will fall and steam turbine output will rise, and β equals 1.

Since the heat load control is achieved directly by adjusting the flow valve of the extracted process steam, there is almost no delay for the resulting steam turbine output variation. Moreover, the duration time of the influence on the output variation rate of steam turbine is the heat load variation time (Δt_{Q}). As a consequence, the $R_{\mathrm{ST}}^{\mathrm{H}}(t)$ can be written as:

$$R_{\mathrm{ST}}^{\mathrm{H}}(t)=\begin{cases} R_{\mathrm{ST}}^{\mathrm{H}} & t_0 < t \le t_0 + \Delta t_{\mathrm{Q}} \\ 0 & t > t_0 + \Delta t_{\mathrm{Q}} \end{cases} \tag{17}$$

$$\Delta t_{\mathrm{Q}} = \frac{\left| Q_{\mathrm{D}} - Q_0 \right|}{R_{\mathrm{H}}} \tag{18}$$

where $R_{\mathrm{ST}}^{\mathrm{H}}$ is the value of the output variation rate of steam turbine caused by the heat load change. Q_{D} and Q_0 are the dispatched heat demand and initial heat load of the plant at the current dispatch time interval, respectively.

Due to the slow heat transfer processes in HRSG, after the gas turbine output variation, there is a period of time delay before the resulting steam turbine output variation in the continuous operation of an NGCC plant [42-45]. The time delay is expressed as Δt_{DE}. Consequently, the steam turbine output variation during the time from t_0 to $t_0+\Delta t_{\mathrm{DE}}$ is caused by the gas turbine output variation during the time from $t_0-\Delta t_{\mathrm{DE}}$ to t_0. Since the time from $t_0-\Delta t_{\mathrm{DE}}$ to t_0 belongs to the previous time interval, the $R_{\mathrm{ST}}^{\mathrm{GT}}$ can be written as:

$$R_{\mathrm{ST}}^{\mathrm{GT}}(t)=\begin{cases} \alpha\gamma R_{\mathrm{ST}}^{\mathrm{GT}} & t_0 < t \le t_0 + \Delta t_{\mathrm{DE}} \\ \alpha R_{\mathrm{ST}}^{\mathrm{GT}} & t > t_0 + \Delta t_{\mathrm{DE}} \end{cases} \tag{19}$$

where $R_{\mathrm{ST}}^{\mathrm{GT}}$ is the value of the output variation rate of steam turbine caused by the gas turbine output change. γ represents the influence degree of the gas turbine output variation in the previous time interval on the steam turbine output variation in the current time interval. The exact value of γ is determined by the specific output variation process of gas turbine during the time from $t_0-\Delta t_{\mathrm{DE}}$ to t_0. The value range of γ at various scenarios of gas turbine output variation is shown in Table. 1.

Table. 1. The value range of γ at various scenarios of gas turbine output variation.

Gas turbine output variation during the time from $t_0-\Delta t_{\mathrm{DE}}$ to t_0	Value range of γ
The gas turbine output continuously changes in the same variation direction as the current time interval.	1
At first the gas turbine output changes in the same variation direction as the current time interval, then it remains unchanged.	(0, 1)
The gas turbine output remains unchanged.	0
At first the gas turbine output changes in the opposite variation direction with the current time interval, then it remains unchanged.	(−1, 0)

The gas turbine output continuously changes in the opposite variation direction with the current time interval.	−1

Substituting Eq. (16) ~ (19) into Eq. (14), then the power load variation capacity (ΔP_C) of an NGCC plant can be calculated as:

$$\begin{aligned}\Delta P_C &= \int_{t_0}^{t_0+\Delta t}\left(\alpha R_{GT}+R_{ST}\right)dt \\ &=\alpha R_{GT}\Delta t+\beta R_{ST}^{H}\Delta t_Q+\alpha\gamma R_{ST}^{GT}\Delta t_{DE}+\alpha R_{ST}^{GT}\left(\Delta t-\Delta t_{DE}\right) \\ &=\alpha R_{GT}\Delta t-R_{ST}^{H}\left(Q_D-Q_0\right)/R_H+\alpha\gamma R_{ST}^{GT}\Delta t_{DE}+\alpha R_{ST}^{GT}\left(\Delta t-\Delta t_{DE}\right)\end{aligned} \tag{20}$$

Based on the various output variation directions of gas turbine, i.e. α, the ΔP_C^{max} ($\alpha = 1$) and ΔP_C^{min} ($\alpha = -1$) can be expressed as:

$$\Delta P_C^{max} = R_{GT}\Delta t-R_{ST}^{H}\left(Q_D-Q_0\right)/R_H+\gamma R_{ST}^{GT}\Delta t_{DE}+R_{ST}^{GT}\left(\Delta t-\Delta t_{DE}\right) \tag{21}$$

$$\Delta P_C^{min} = -R_{GT}\Delta t-R_{ST}^{H}\left(Q_D-Q_0\right)/R_H-\gamma R_{ST}^{GT}\Delta t_{DE}-R_{ST}^{GT}\left(\Delta t-\Delta t_{DE}\right) \tag{22}$$

The schematic diagram of ΔQ_C and ΔP_C in the general LVC model and advanced LVC model of an NGCC plant is shown in Fig. 1. In this work, the area enclosed by the LVC model is defined as the relative feasible operating zone (ΔFOZ). The shaded areas in the upper right and lower left corners of the ΔFOZ are the loads variation range that is feasible in the general LVC model, but unfeasible in the advanced LVC model. If the CHPDED model with general LVC models is applied in actual operation, some required loads variations in the calculation result may be located in the shaded areas, so that the corresponding dispatched demands cannot be reached in time. This will further break the balance between generation and demands of the NGCC station, which is harmful to the operational reliability and security.

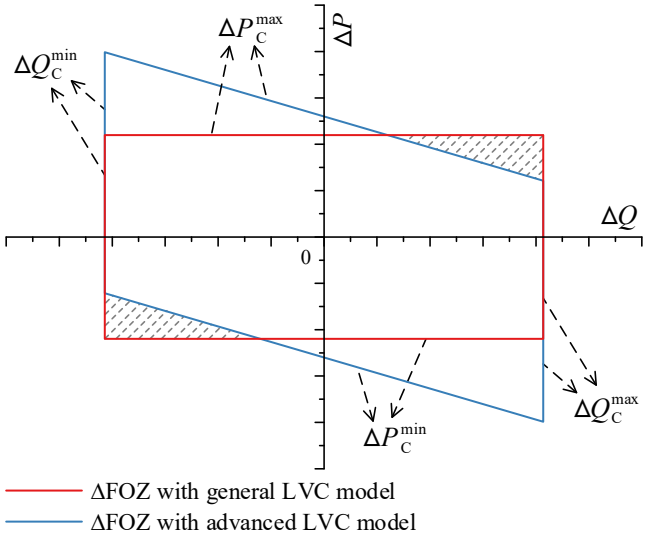

Fig. 1. Schematic diagram of ΔFOZs with general LVC model and advanced LVC model of an NGCC plant.

In addition, when $\Delta t < \Delta t_{DE}$, the formulations of the ΔP_C^{max} and ΔP_C^{min} are:

$$\Delta P_C^{max} = R_{GT}\Delta t-R_{ST}^{H}\left(Q_D-Q_0\right)/R_H+\gamma R_{ST}^{GT}\Delta t \tag{23}$$

$$\Delta P_{\mathrm{C}}^{\min} = -R_{\mathrm{GT}}\Delta t - R_{\mathrm{ST}}^{\mathrm{H}}\left(Q_{\mathrm{D}} - Q_0\right)/R_{\mathrm{H}} - \gamma R_{\mathrm{ST}}^{\mathrm{GT}}\Delta t \tag{24}$$

2.3 Simplification of the advanced LVC model for CHPDED calculation

In the CHPDED calculation, if the general LVC model is adopted in the constraints (3), then Eq. (12) and (13) are substituted into Eq. (6). If the advanced LVC model is adopted in the constraints (3), then Eq. (21) and (22) are substituted into Eq. (6). In Eq. (21) and (22), R_{H}, R_{GT}, $R_{\mathrm{ST}}^{\mathrm{H}}$, $R_{\mathrm{ST}}^{\mathrm{GT}}$ and Δt_{DE} are the operational characteristic parameters of an NGCC plant, which have been determined before the CHPDED calculation. Q_{D} is the dispatched heat demand generated at the current dispatch time interval, which can be directly obtained during the calculation. In contrast, the determination of the exact value of γ is very complicated in theory.

As mentioned above, γ represents the influence degree of the gas turbine output variation in the previous time interval on the steam turbine output variation in the current time interval. The exact value of γ is determined by the specific output variation process of gas turbine during the last Δt_{DE} time in the previous time interval. This requires the dynamic simulation of the plant operation process in the previous time interval based on the field power and heat loads control logic of an NGCC plant. The studies [42-50] showed that the computational complexity of the dynamic simulation model of an NGCC plant was very large. If the dynamic simulation model is integrated into the CHPDED model, it will lead to a huge computational burden. Therefore, considering the computational burden of the CHPDED model, the determination of the exact value of γ is simplified based on the field operational data in this work. The detailed simplification process is elaborated below. By defining $\Delta P = P_{\mathrm{D}}(t) - P_{\mathrm{D}}(t-1)$, Eq. (6) in the constraints (3) can be written as:

$$\Delta P_{\mathrm{C}}^{\min} \le \Delta P \le \Delta P_{\mathrm{C}}^{\max} \tag{25}$$

Substituting Eq. (21) and (22) into Eq. (25), then it can be deduced that:

$$-R_{\mathrm{GT}}\Delta t - R_{\mathrm{ST}}^{\mathrm{H}}\left(Q_{\mathrm{D}} - Q_0\right)/R_{\mathrm{H}} - \gamma R_{\mathrm{ST}}^{\mathrm{GT}}\Delta t_{\mathrm{DE}} - R_{\mathrm{ST}}^{\mathrm{GT}}\left(\Delta t - \Delta t_{\mathrm{DE}}\right) \le \Delta P \tag{26}$$

$$\gamma \ge \frac{-\Delta P - R_{\mathrm{GT}}\Delta t - R_{\mathrm{ST}}^{\mathrm{H}}\left(Q_{\mathrm{D}} - Q_0\right)/R_{\mathrm{H}} - R_{\mathrm{ST}}^{\mathrm{GT}}\left(\Delta t - \Delta t_{\mathrm{DE}}\right)}{R_{\mathrm{ST}}^{\mathrm{GT}}\Delta t_{\mathrm{DE}}} \tag{27}$$

$$\Delta P \le R_{\mathrm{GT}}\Delta t - R_{\mathrm{ST}}^{\mathrm{H}}\left(Q_{\mathrm{D}} - Q_0\right)/R_{\mathrm{H}} + \gamma R_{\mathrm{ST}}^{\mathrm{GT}}\Delta t_{\mathrm{DE}} + R_{\mathrm{ST}}^{\mathrm{GT}}\left(\Delta t - \Delta t_{\mathrm{DE}}\right) \tag{28}$$

$$\gamma \ge \frac{\Delta P - R_{\mathrm{GT}}\Delta t + R_{\mathrm{ST}}^{\mathrm{H}}\left(Q_{\mathrm{D}} - Q_0\right)/R_{\mathrm{H}} - R_{\mathrm{ST}}^{\mathrm{GT}}\left(\Delta t - \Delta t_{\mathrm{DE}}\right)}{R_{\mathrm{ST}}^{\mathrm{GT}}\Delta t_{\mathrm{DE}}} \tag{29}$$

In the meanwhile, the definition of γ shows that $-1 \le \gamma \le 1$. Combining Eq. (27) and (29), then it can be deduced that:

$$\gamma^{\min} \le \gamma \le 1 \tag{30}$$

$$\gamma^{\min} = \max\left\{\gamma_1, \gamma_2, -1\right\} \tag{31}$$

$$\gamma_1 = \frac{-\Delta P - R_{GT}\Delta t - R_{ST}^{H}\left(Q_D - Q_0\right)/R_H - R_{ST}^{GT}\left(\Delta t - \Delta t_{DE}\right)}{R_{ST}^{GT}\Delta t_{DE}} \tag{32}$$

$$\gamma_2 = \frac{\Delta P - R_{GT}\Delta t + R_{ST}^{H}\left(Q_D - Q_0\right)/R_H - R_{ST}^{GT}\left(\Delta t - \Delta t_{DE}\right)}{R_{ST}^{GT}\Delta t_{DE}} \tag{33}$$

When $\Delta t < \Delta t_{DE}$, the formulations of the γ_1 and γ_2 are:

$$\gamma_1 = \frac{-\Delta P - R_{GT}\Delta t - R_{ST}^{H}\left(Q_D - Q_0\right)/R_H}{R_{ST}^{GT}\Delta t} \tag{34}$$

$$\gamma_2 = \frac{\Delta P - R_{GT}\Delta t + R_{ST}^{H}\left(Q_D - Q_0\right)/R_H}{R_{ST}^{GT}\Delta t} \tag{35}$$

From Eq. (21) and (22), it can be seen that the smaller γ is, the smaller power load variation capacity is. Thus, in this work, for the sake of higher feasibility of the dispatched demands, γ is set to γ^{min} ($\gamma = \gamma^{min}$) in the CHPDED model with advanced LVC models. Then the field operational data of NGCC plants is substituted into Eq. (32) and (33), and the γ^{min} at various Δt can be calculated. The logic diagram of the CHPDED model with advanced LVC models of NGCC plants is shown in Fig. 2.

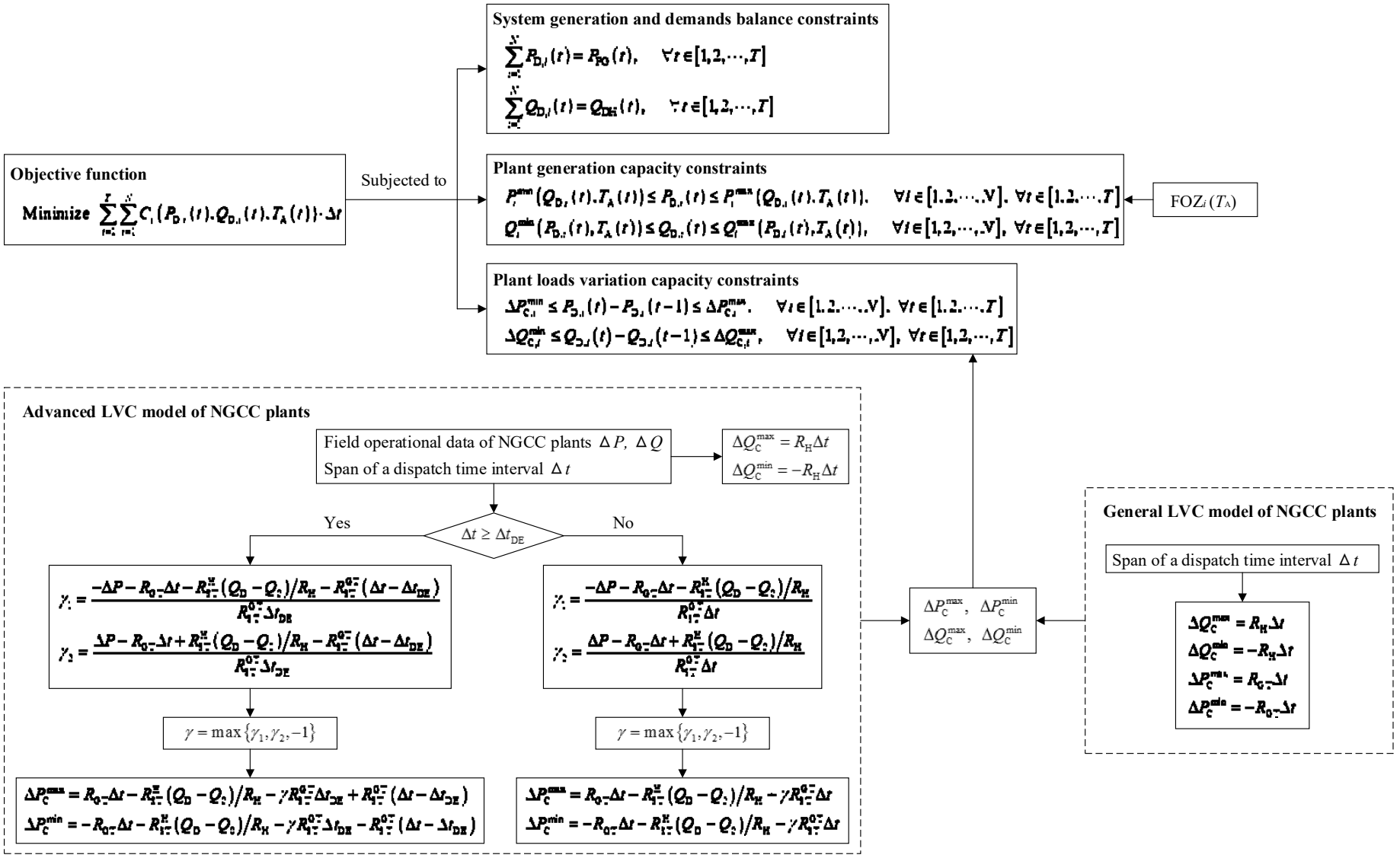

Fig. 2. Logic diagram of the CHPDED models with general LVC models and advanced LVC models of NGCC plants.

3 Case description

3.1 Reference NGCC station

In this work, an NGCC station comprised of one 1×1 plant and one 2×1 plant is taken as the reference system. The NGCC station is located in North China, and the local ambient temperature annually ranges from -10 °C to 38 °C. Every gas turbine in both plants is Siemens SGT5-4000F and equipped with a triple pressure reheat sub-critical HRSG. Two steam turbines are both composed of a high pressure cylinder, an intermediate pressure cylinder and a low pressure cylinder. In each steam turbine, the process steam supplied to DH heaters is extracted from the intermediate pressure cylinder exhaust steam. The configuration of these two plants is shown in Fig. 3, and the nominal values of technical parameters are summarized in Section S1 in supplementary material.

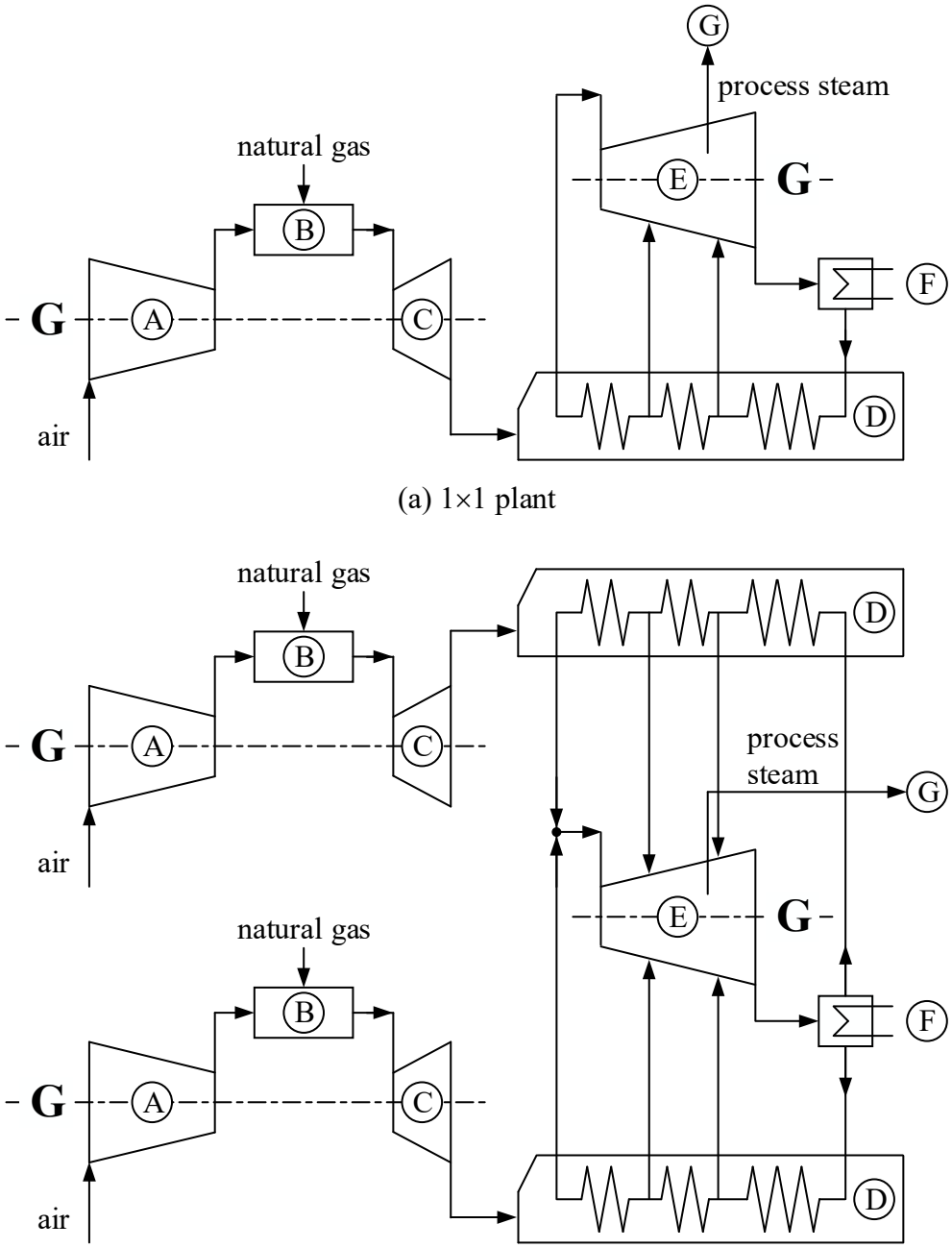

Fig. 3. Schematic diagrams of the 1×1 plant and the 2×1 plant at CHP mode.

As presented in Section 2, the operational characteristic parameters of NGCC plants used in the CHPDED calculation include: the plant heat load ramp rate (R_{H}), the output variation rate of gas turbine (R_{GT}), the delay time between the gas turbine output variation and the resulting steam turbine output variation (Δt_{DE}), the output variation rate of steam turbine caused by the gas turbine output variation ($R_{\mathrm{ST}}^{\mathrm{GT}}$), the output variation rate of steam turbine caused by the heat load variation ($R_{\mathrm{ST}}^{\mathrm{H}}$), the FOZ, and the fuel consumption characteristic. The values of these parameters of the two reference plants used in

the calculation cases are shown in Table. 2. The description on the source and assignment process of these parameter values is elaborated in Section S2 in supplementary material.

Table. 2. Operational characteristic parameters of the two reference NGCC plants used in the calculation cases.

Parameter	Value	
	1x1	2x1
R_{H}	19.7 MW/min	57.5 MW/min
R_{GT}	11 MW/min	22 MW/min (2 gas turbines)
Δt_{DE}	6.5 minutes	3.5 minutes
$R_{\mathrm{ST}}^{\mathrm{GT}}$	2.5 MW/min	4 MW/min
$R_{\mathrm{ST}}^{\mathrm{H}}$	5.0 MW/min	13.9 MW/min
FOZ	Fig. 4	Fig. 4
Fuel consumption characteristic	LSSVR model	LSSVR model

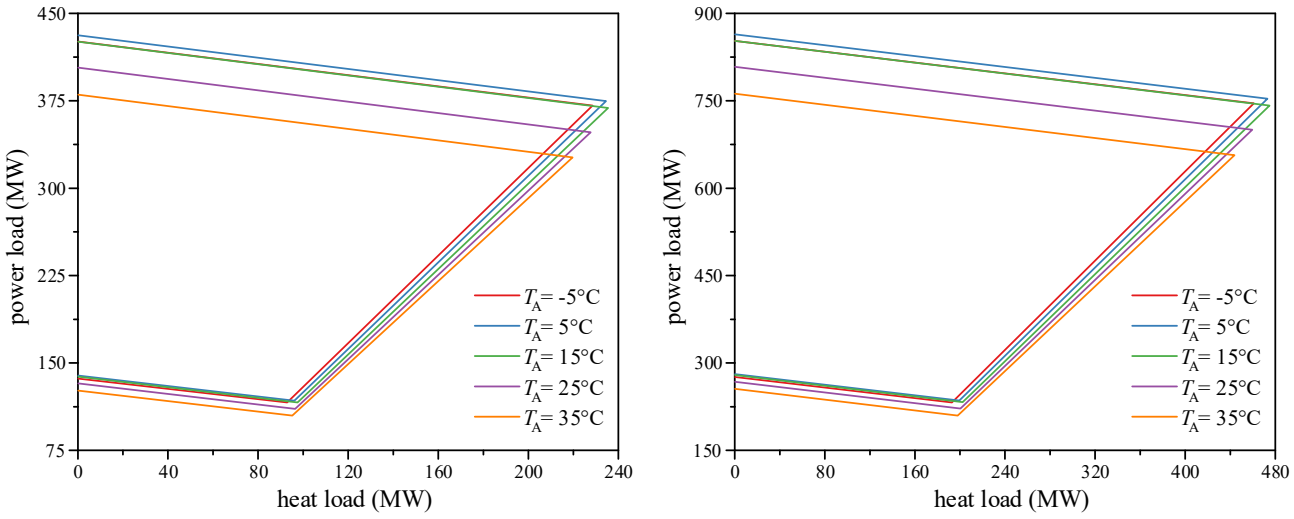

(a) 1×1 plant (b) 2×1 plant

Fig. 4. FOZs of the two reference plants at various ambient temperature.

3.2 Basic information of calculation cases

In order to investigate the influence of different LVC models of NGCC plants, the CHPDED calculation is performed on the daily demand scenario with general LVC models and advanced LVC models, respectively. The historical operational data of the reference NGCC station on the typical day of each month in the last winter is taken to generate the demand scenarios. The four typical days are November 7th, December 18th, January 8th, and February 19th. The field power and heat demands of the NGCC station on the typical days are utilized to simulate the day-ahead demands forecast with the resolution of 5 minutes in the CHPDED calculation. According to Eq. (1), the objective function of the CHPDED model for the reference NGCC station can be written as:

$$\text{Minimize} \sum_{t=1}^{288}\left[C_1\left(P_{\mathrm{D},1}(t),Q_{\mathrm{D},1}(t),T_{\mathrm{A}}(t)\right)+C_2\left(P_{\mathrm{D},2}(t),Q_{\mathrm{D},2}(t),T_{\mathrm{A}}(t)\right)\right]\cdot\Delta t \quad (36)$$

where the number in subscripts represents the two plants, 1 for 1×1 plant and 2 for 2×1 plant. The optimization variables are the power and heat demands of the two plants at each dispatch time interval, i.e. $P_{D,1}(t)$, $Q_{D,1}(t)$, $P_{D,2}(t)$ and $Q_{D,2}(t)$. Based on the system generation and demands balance constraints, the boundary conditions of the CHPDED calculation are the power and heat demands of the NGCC station, and ambient temperature at each dispatch time interval. The curves of these three parameters on the four typical days are shown in Fig. 5. The power demands of the station are from the power grid, represented by $P_{PG}(t)$ in Eq. (2). The heat demands of the station are from the DH system, represented by $Q_{DH}(t)$ in Eq. (3).

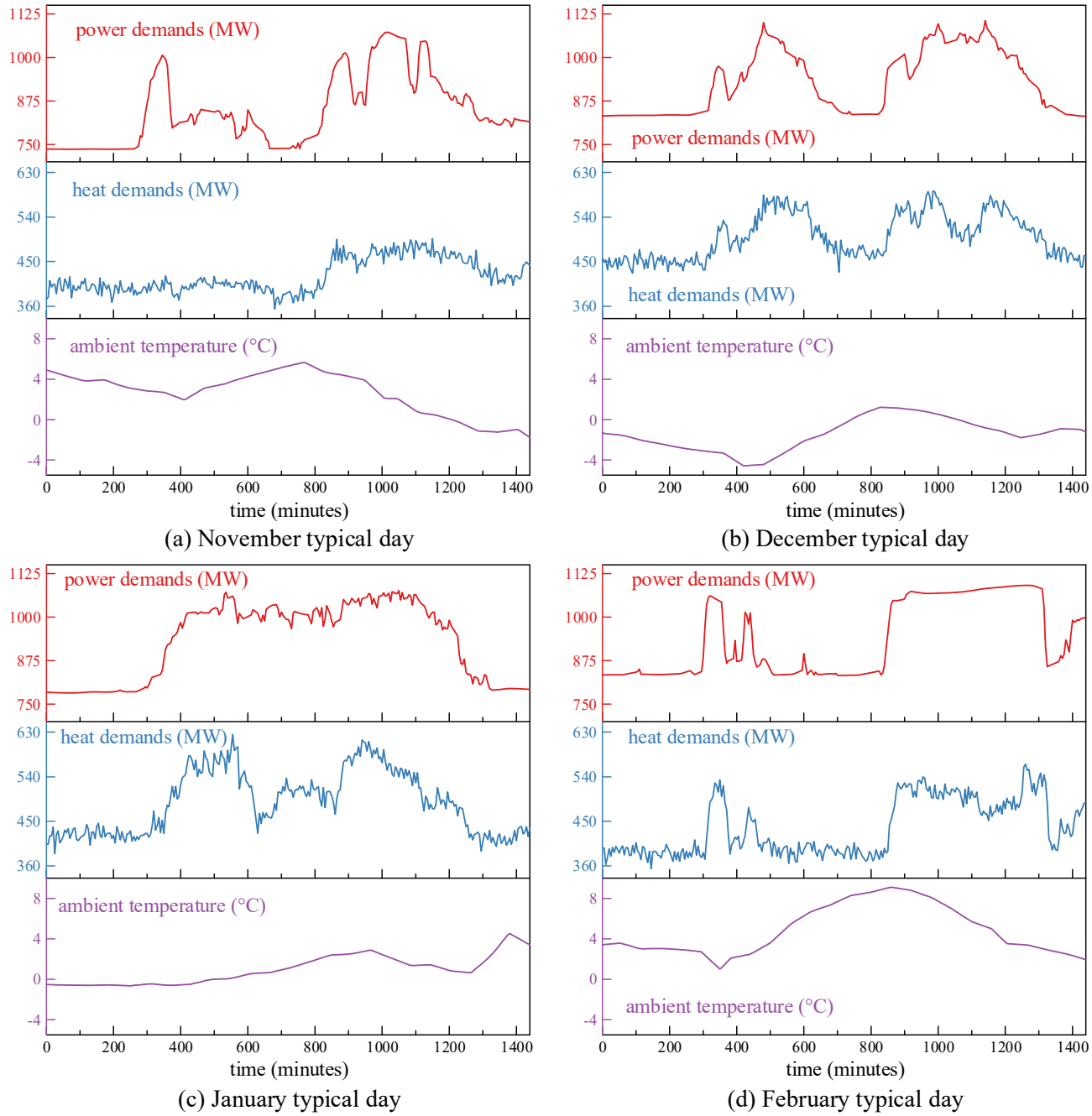

Fig. 5. Power and heat demands of the NGCC station, and ambient temperature on the four typical days.

Based on the field operational data of the two NGCC plants on the four typical days, the field loads

variations at various time spans (Δt) can be calculated. The field loads variations (ΔP and ΔQ) at the time span of 5 minutes are shown in Fig. 6. For each NGCC plant, the field loads variations can be substituted into Eq. (31) ~ (33) to calculate the value of γ in the advanced LVC model. The values of γ of the 1×1 plant and the 2×1 plant at the time span of 5 minutes are −0.26 and 0.62, respectively. Then the ΔP_C^{max} and ΔP_C^{min} of the two plants in the constraints (3) of the CHPDED model are calculated according to Eq. (21) and (22). In addition, it also can be seen from the Fig. 6 that some field loads variations are located outside the ΔFOZ with general LVC model. This indicates that the general LVC model is not able to represent the actual loads variation capacity of NGCC plants accurately.

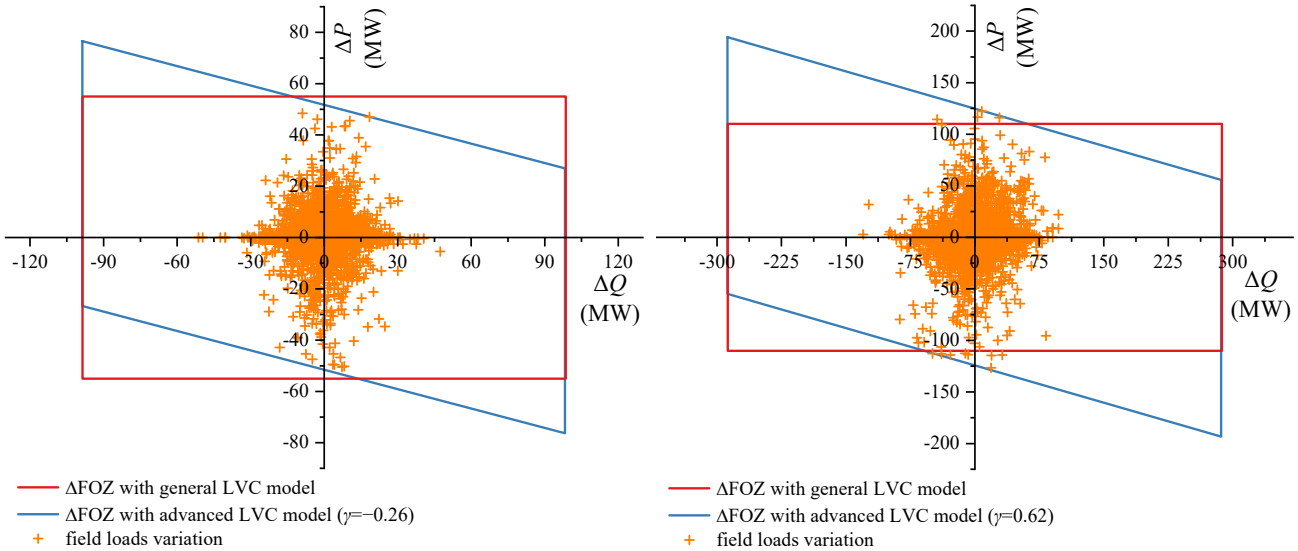

(a) 1×1 plant (b) 2×1 plant

Fig. 6. Field loads variation data of the two plants at the time span of 5 minutes.

4 Results and discussion

In this work, a particle swarm optimization algorithm with chaos searching technique (CST-PSO) [52,53] is employed to calculate CHPDED models. The CST-PSO is a heuristic optimization algorithm with excellent performance in solving optimization problems, especially for complex engineering scenarios [53-56]. The chaos searching technique is integrated into the particle swarm optimization algorithm to improve the particle position update process, so that higher accuracy and robustness of the algorithm are achieved. In the literature [53-55], the performance of the CST-PSO algorithm was tested on some benchmark problems, and the test results proved its efficiency and reliability.

4.1 Demand scenarios of typical days

For illustrating the influence of various LVC models of NGCC plants, the CHPDED models with general LVC models and advanced LVC models are calculated on the demand scenarios of the four typical days presented in Section 3, respectively. Based on the CHPDED calculation result, the required loads variation of each plant at each dispatched time interval is calculated and showed on the ΔFOZ. The demand scenario of the November typical day is taken as an instance to display. The required loads variations of the two plants at each dispatch time interval in the calculation result of the CHPDED model with general LVC models are shown in Fig. 7. It can be seen that there are 63 required loads variations of the 1×1 plant located in the upper right and lower left corners of the ΔFOZ. These

required loads variations exceed the actual loads variation capacity of the plant, with the result that the corresponding dispatched demands are unfeasible. This may further lead to the demands from the power grid failing to meet in time. There are even 20 required loads variations of the 1×1 plant exceeding its theoretical maximum loads variation capacity, which is represented by the advanced LVC model with $\gamma = 1$. The required loads variations of the two plants at each dispatch time interval in the calculation result of the CHPDED model with advanced LVC models are shown in Fig. 8. It can be seen that all the required loads variations are within the actual loads variation capacity of the plants. In addition, there are some required loads variations located in the upper left and lower right corners of the ΔFOZ, which are inside the advanced LVC model, but outside the general LVC model. This indicates that the influence of heat load variation process on power load adjustment process can be utilized in the CHPDED model with advanced LVC models to achieve a better dispatch result. The required loads variations in the CHPDED calculation results of the demand scenarios of the other three typical days are similar to those in the CHPDED calculation results of the demand scenario of the November typical day (Fig. 7 and Fig. 8), and are presented in Section S3 in supplementary material.

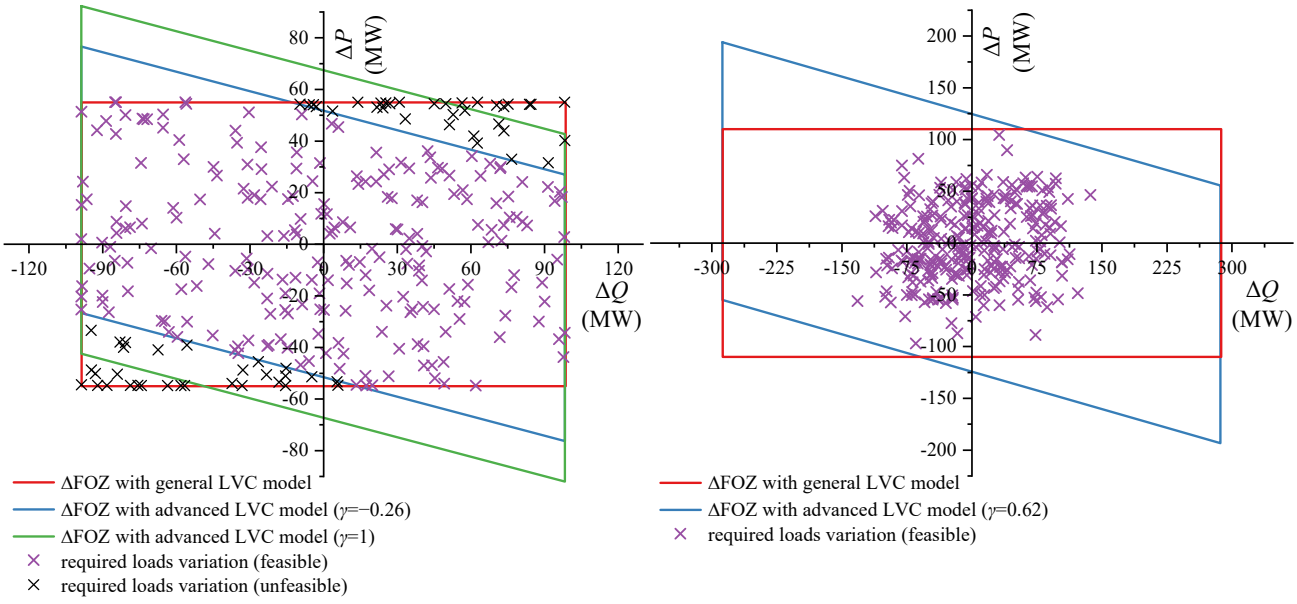

(a) 1×1 plant (b) 2×1 plant

Fig. 7. Required loads variations of the two plants in the calculation result of the CHPDED model with general LVC models. (Demand scenario of the November typical day is taken as an instance)

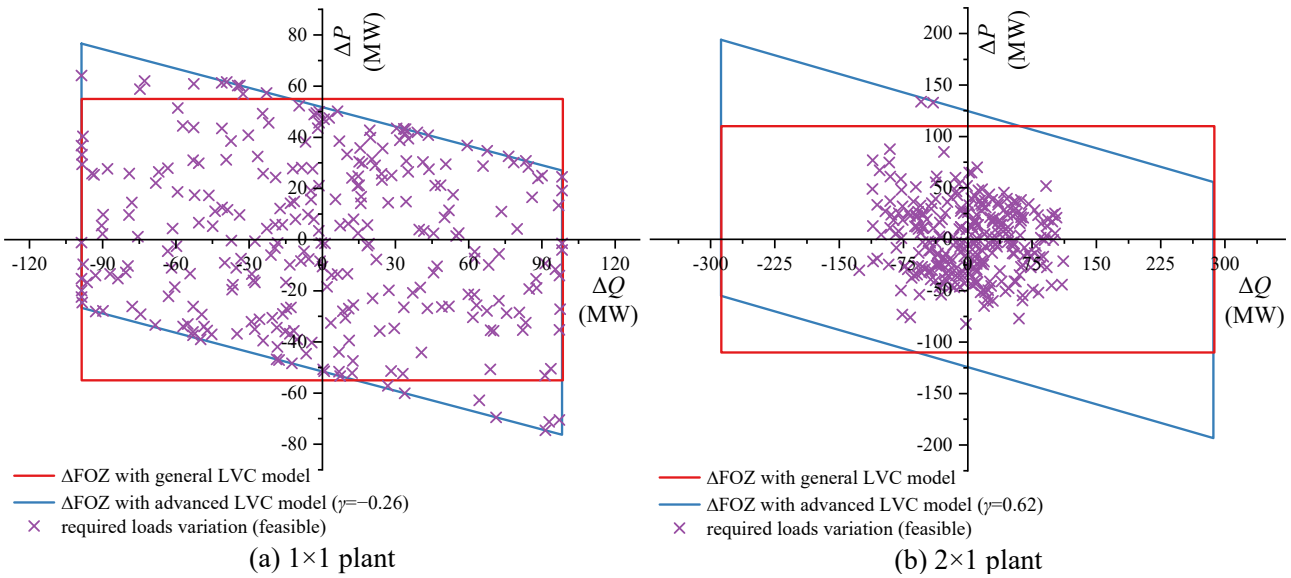

(a) 1×1 plant (b) 2×1 plant

Fig. 8. Required loads variations of the two plants in the calculation result of the CHPDED model with advanced LVC models. (Demand scenario of the November typical day is taken as an instance)

One interesting phenomenon is that both in the calculation results of the CHPDED models with general LVC models and advanced LVC models, there are several dispatched demands of the 1×1 plant located on the boundary of the ΔFOZ, as shown in Fig. 7(a) and Fig. 8(a). In contrast, there are few dispatched demands of the 2×1 plant located on the boundary of the ΔFOZ. The reason for this phenomenon may be the small loads variation capacity of the 1×1 plant. To verify this conjecture, parameters of the advanced LVC model of the 1×1 plant are assumed to be the other two cases, and the CHPDED calculation is performed again. In the Case 1, the loads variation capacity of the 1×1 plant is set to the same as that of the 2×1 plant. In the Case 2, no constraints are imposed on the loads variation capacity of the 1×1 plant. The amount of the dispatched demands of the two plants that are located on the boundary of their ΔFOZs is counted, as shown in Table. 3. It can be seen that with the loads variation capacity of the 1×1 plant becoming larger, the amount of the dispatched demands of the 1×1 plant that are located on the boundary of its ΔFOZ shrinks. In comparison, more dispatched demands of the 2×1 plant are located on the boundary of its ΔFOZ, and the conjecture is proved.

Table. 3. Amount of the dispatched demands of the two plants that are located on the boundary of their ΔFOZs in the calculation results of the CHPDED model with advanced LVC models.

Demand scenario	Benchmark case*		Case1*		Case2*	
	1×1 plant	2×1 plant	1×1 plant	2×1 plant	1×1 plant	2×1 plant
November typical day	48	1	3	5	-	10
December typical day	20	0	5	3	-	4
January typical day	16	0	6	6	-	8
February typical day	57	0	3	6	-	11

Benchmark case*: actual loads variation capacity of the 1×1 plant.

Case1*: loads variation capacity of the 1×1 plant is set to the same as that of the 2×1 plant.

Case2*: no constraints are imposed on the loads variation capacity of the 1×1 plant.

In order to demonstrate the improvement in the operational economic performance, the total fuel consumption of the NGCC station is calculated for the field operational demands of plants and the dispatched demands of the CHPDED model with advanced LVC models, respectively. The fuel consumption is calculated based on the fuel consumption model of each plant. As can be seen from Table. 4, the CHPDED model with advanced LVC models can save the total fuel consumption by approximately 0.11% to 0.26% over the field operational demands of plants. Among the demand scenarios of the four typical days, the fuel consumption saving is relatively large on the November and February typical days, and relatively small on the December and January typical days. The reason for this phenomenon is that the demands of the power station on the December and January typical days are located closer to the boundary of the FOZ of the power station, as shown in Fig. 9. The boundary of the FOZ of the power station is the combination of the boundary operating conditions of plants, which refer to the operating conditions under the maximum or minimum gas turbine output, and the operating conditions under the maximum or minimum flow of extracted process steam. When a demand of the power station is located closer to the boundary of its FOZ, the adjustment scope for the demands of plants, i.e. the dispatch scope of the CHPDED model, is smaller under the constraints of system generation and demands balance. Therefore, the improvement in the operational economic performance is small on the demand scenarios of the December and January typical days. In conclusion, compared with CHPDED models in the existing research, the CHPDED model with advanced LVC models significantly improves the feasibility of dispatched demands, which benefits a lot for the operational reliability of plants. For the operators of an NGCC station, the CHPDED model with advanced LVC models is more credible to put into real utilization. The improvement on the economic performance from CHPDED could be really achieved in the field operation of the NGCC station.

Table. 4. Total fuel consumption of the NGCC station on the four typical days.

Demand scenario	Total fuel consumption of the NGCC station ($\times 10^6$ kg)		Saving (%)
	Field operational demands of plants	CHPDED model with advanced LVC models	
November typical day	3.253	3.245	0.246
December typical day	3.557	3.552	0.141
January typical day	3.546	3.542	0.113
February typical day	3.513	3.504	0.256

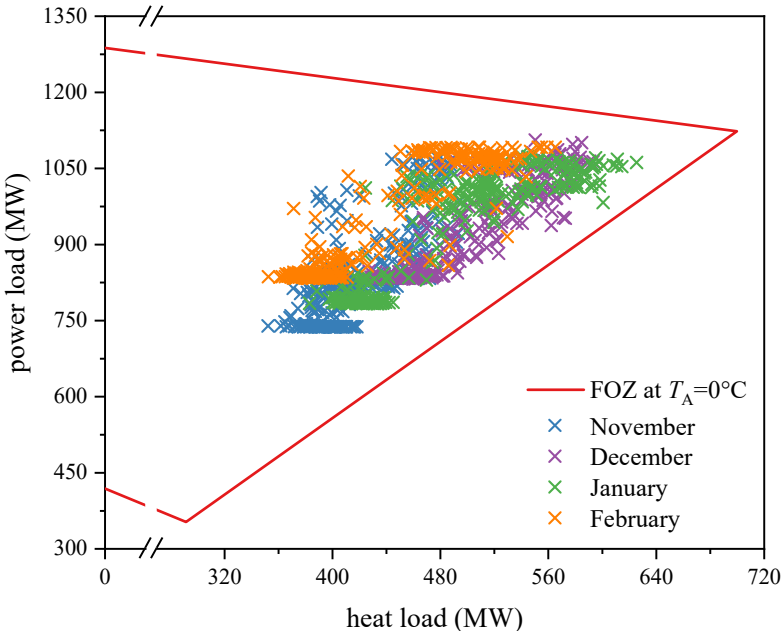

Fig. 9. Locations on the FOZ of the demands of the power station on the four typical days.

4.2 Future demand scenarios

In recent years, with the rapid development of various energy technologies such as electricity generation of renewable energy and heat pumps, the demand scenario changes frequently. Three future demand scenarios are assumed in this work to test the applicability and necessity of the CHPDED model with advanced LVC models. Some modifications are performed on the demand scenarios of the typical days to represent the three future demand scenarios, which are elaborated as follows:

(1) Demand scenario S1: a large amount of electricity generated from the intermittent renewable energy, such as wind power and photovoltaic power, will be connected to the power grid [57-59]. On the demand-side, electric vehicles will take a major share of the market [60-63]. Both trends will lead to greater fluctuation amplitude of power demands for the NGCC station. To simulate this demand scenario, the fluctuation amplitude of power demands in the demand scenarios of the typical days is increased to 1.3 times, with total daily power generation and heat demands unchanged. The power demands curve in the demand scenario S1 of the November typical day is shown in Fig. 10 as an instance.

(2) Demand scenario S2: heat pumps will be widely utilized in the heating sector, in which electricity is used to take heat from sources like ambient air, water, or ground [64,65]. As a result, for the NGCC station, heat demands will decrease while power demands will increase. To simulate this demand scenario, 50% heat demand is converted into power demand with the heat pumps' coefficient of performance (COP), which is set to 4 according to the literature [64,65]. The power and heat demands curves in the demand scenario S2 of the November typical day are shown in Fig. 11 as an instance.

(3) Demand scenario S3: with the development of demands forecast algorithms and technology, the resolution of the day-ahead demands forecast will be higher. To simulate this demand scenario, the span of a dispatch time interval is reduced to 2 minutes. Based on the field operational data on the typical days, loads variations of the two NGCC plants at the time span

of 2 minutes are shown in Fig. 12. The values of γ of the 1×1 plant and the 2×1 plant are calculated as 0.59 and 0.96, respectively. There are more field loads variations located outside the general LVC model. It further proves that the general LVC model is not able to represent the actual loads variation capacity of NGCC plants accurately.

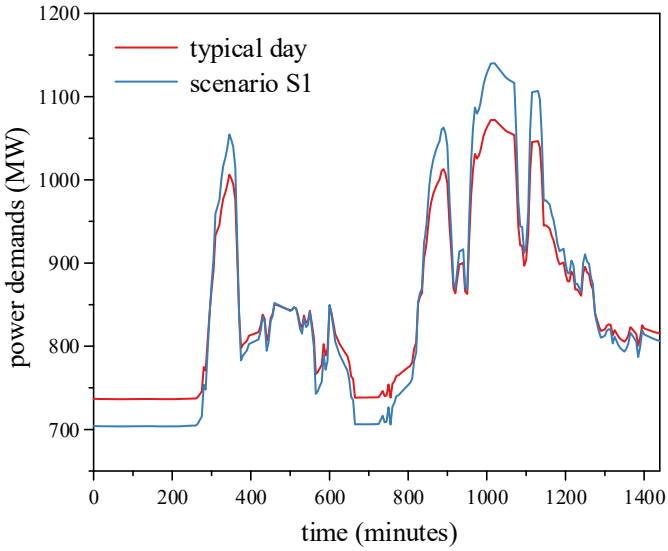

Fig. 10. Power demands of the NGCC station in the demand scenario S1 of the November typical day.

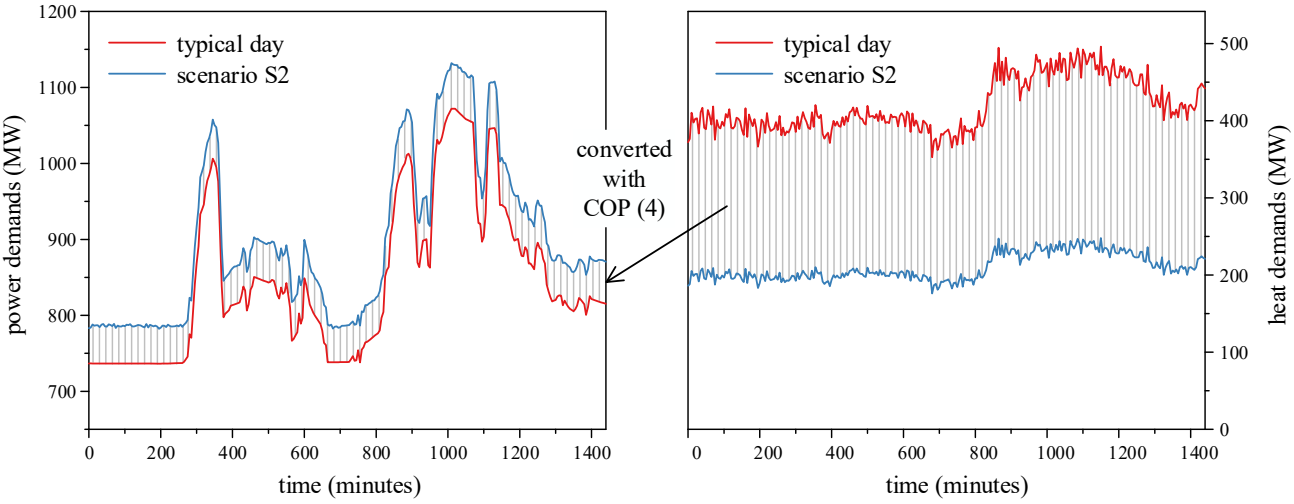

Fig. 11. Power and heat demands of the NGCC station in the demand scenario S2 of the November typical day.

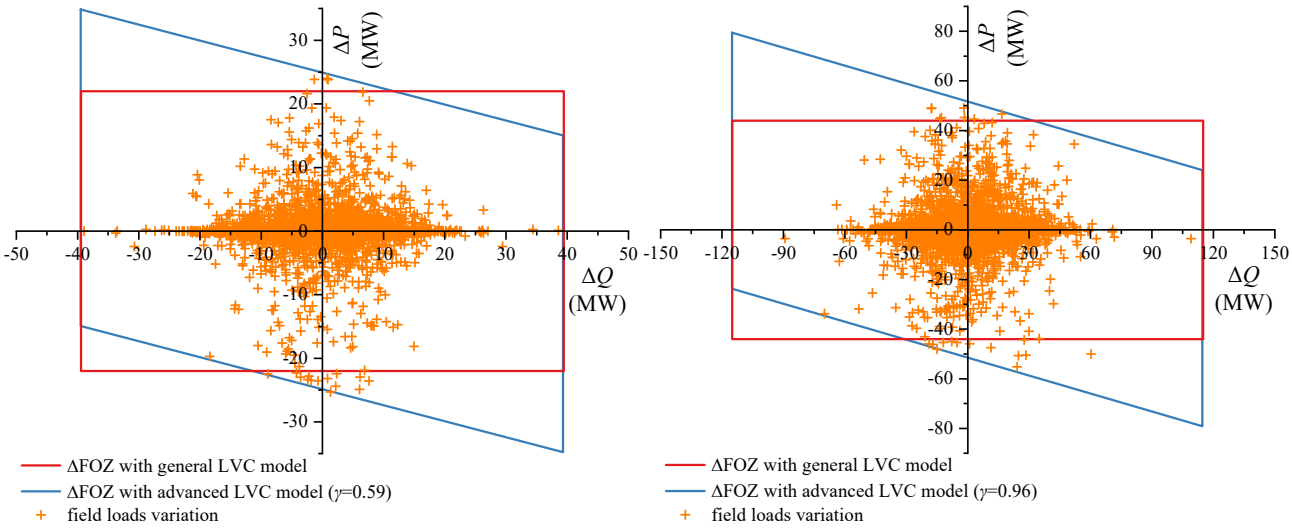

(a) 1×1 plant (b) 2×1 plant

Fig. 12. Field loads variation data of the two plants at the time span of 2 minutes.

The CHPDED models with general LVC models and advanced LVC models are calculated on the above three future demand scenarios, respectively. The amount of the unfeasible dispatched demands in the calculation results is counted and shown in Table. 5. It can be seen that, on the one hand, under the three future demand scenarios, there are no unfeasible dispatched demands in the calculation results of the CHPDED model with advanced LVC models. The applicability of the CHPDED model with advanced LVC models is well proved. On the other hand, in the calculation results of the CHPDED model with general LVC models, the amount of the unfeasible dispatched demands under the future demand scenarios S1 and S3 is larger than that under the demand scenarios of the typical days. This indicates that in these two future demand scenarios, the CHPDED model with advanced LVC models is needed more urgently to guarantee the operational reliability and security of NGCC plants.

Table. 5. Amount of the unfeasible dispatched demands in the CHPDED calculation results under the three future demand scenarios.

Demand scenario	LVC models used in CHPDED calculation	November typical day	December typical day	January typical day	February typical day
Typical day	general LVC models	63	60	53	79
	advanced LVC models	0	0	0	0
S1	general LVC models	76	68	65	86
	advanced LVC models	0	0	0	0
S2	general LVC models	13	22	41	39
	advanced LVC models	0	0	0	0
S3	general LVC models	90	81	96	139
	advanced LVC models	0	0	0	0

5 Conclusions

In this study, based on the actual operational characteristics of an NGCC plant at CHP mode, a plant advanced LVC model is developed. The advanced LVC models of NGCC plants are integrated

into the CHPDED model to guarantee the feasibility of dispatched demands. In addition, considering the computational burden of the CHPDED model, a field operational data based simplification method for the advanced LVC model is presented. The field operational data of an actual NGCC station is taken to perform case studies for testing LVC models of plants and CHPDED models. The CHPDED model in the existing research and the CHPDED model with advanced LVC models are calculated on several demand scenarios, respectively. Further, the comparison and analysis of the calculation results are carried out.

The field operational data of the reference NGCC station on four typical days in the winter of 2019 and 2020 is utilized to simulate the day-ahead demands forecast with the resolution of 5 minutes in the CHPDED calculation. In the calculation results of the CHPDED model in the existing research, approximately 64 dispatched demands exceed the actual loads variation capacity of plants. The calculation results of the CHPDED model with advanced LVC models show that all the dispatched demands are feasible. Moreover, the influence of the heat load variation process on the power load adjustment process is employed in the CHPDED model with advanced LVC models to achieve better dispatch results. In the calculation cases of this study, the CHPDED model with advanced LVC models could save the total fuel consumption by approximately 0.11% to 0.26% over the field operational demands. CHPDED calculation is also performed on three future demand scenarios. In the future energy context of lots of intermittent renewable energy connected to the power grid, electric vehicles widely used, and higher resolution of demands forecast, the necessity of the CHPDED model with advanced LVC models is further highlighted. In comparison with CHPDED models in the existing research, the CHPDED model with advanced LVC models shows a great improvement on the feasibility of the dispatched demands, which benefits a lot for the operational reliability of plants. For the operators of an NGCC station, the CHPDED model with advanced LVC models is more credible to put into real utilization, thereby enhancing the actual application value of CHPDED in the field operation.

Nomenclature

Acronyms	
CHP	combined heat and power
CHPDED	combined heat and power dynamic economic dispatch
COP	coefficient of performance
CST-PSO	particle swarm optimization algorithm with chaos searching technique
DH	district heating
FOZ	feasible operating zone
HRSG	heat recovery steam generator
LSSVR	least square support vector regression
LVC	loads variation capacity
NGCC	natural gas combined cycle
Symbol	
C	plant fuel consumption function
P	power demand / load
Q	heat demand / load
R	load ramp rate / output variation rate
T	temperature
α	output variation direction of gas turbine
β	output variation direction of steam turbine caused by the heat load change
γ	influence degree of the gas turbine output variation in the previous time interval on the steam turbine output variation in the current time interval
Subscripts	
A	ambient
C	capacity
D	dispatched demand
DE	delay
DH	district heating system
GT	gas turbine
H	heat load
i	number of NGCC plants
PG	power grid
ST	steam turbine

Acknowledgements

This study was supported by the National Natural Science Foundation of China (grant numbers 51976031), the Fundamental from China Scholarship Council (grant numbers 201906090046) and the Qinglan Project of Jiangsu Province, China.

References

[1] Nord L O, Bolland O. Carbon Dioxide Emission Management in Power Generation[M]. John Wiley & Sons, 2020.

[2] Rúa J, Nord L O. Optimal control of flexible natural gas combined cycles with stress monitoring: Linear vs nonlinear model predictive control[J]. Applied Energy, 2020, 265: 114820.

[3] Wang Y, Wang Y, Huang Y, et al. Planning and operation method of the regional integrated energy system considering economy and environment[J]. Energy, 2019, 171: 731-750.

[4] Lu S, Gu W, Zhou S, et al. High resolution modeling and decentralized dispatch of heat and electricity integrated energy system[J]. IEEE Transactions on Sustainable Energy, 2019.

[5] Zhou J, Wu Y, Wu C, et al. A hybrid fuzzy multi-criteria decision-making approach for performance analysis and evaluation of park-level integrated energy system[J]. Energy Conversion and Management, 2019, 201: 112134.

[6] Wang J, You S, Zong Y, et al. Flexibility of combined heat and power plants: A review of technologies and operation strategies[J]. Applied Energy, 2019, 252: 113445.

[7] Nazari-Heris M, Mohammadi-Ivatloo B, Asadi S, et al. Large-scale combined heat and power economic dispatch using a novel multi-player harmony search method[J]. Applied Thermal Engineering, 2019, 154: 493-504.

[8] Noussan M, Jarre M, Roberto R, et al. Combined vs separate heat and power production–Primary energy comparison in high renewable share contexts[J]. Applied Energy, 2018, 213: 1-10.

[9] Gonzalez-Salazar M A, Kirsten T, Prchlik L. Review of the operational flexibility and emissions of gas-and coal-fired power plants in a future with growing renewables[J]. Renewable and Sustainable Energy Reviews, 2018, 82: 1497-1513.

[10] Gui-Xiong H E, Yan H, Chen L, et al. Economic dispatch analysis of regional Electricity–Gas system integrated with distributed gas injection[J]. Energy, 2020: 117512.

[11] Zheng L, Zhou X, Qiu Q, et al. Day-ahead optimal dispatch of an integrated energy system considering time-frequency characteristics of renewable energy source output[J]. Energy, 2020, 209: 118434.

[12] Collins S, Deane J P, Poncelet K, et al. Integrating short term variations of the power system into integrated energy system models: A methodological review[J]. Renewable and Sustainable Energy Reviews, 2017, 76: 839-856.

[13] Ma H, Xu F, Chen Q, et al. Dispatch framework of power system with heat storage facilities in combined heat and power plants for wind power accommodation[J]. IET Renewable Power Generation, 2019, 14(3): 335-343.

[14] Zhou Y, Zhao P, Xu F, et al. Optimal Dispatch Strategy for a Flexible Integrated Energy Storage System for Wind Power Accommodation[J]. Energies, 2020, 13(5): 1073.

[15] Deng B, Teng Y, Hui Q, et al. Real-Coded Quantum Optimization-Based Bi-Level Dispatching

Strategy of Integrated Power and Heat systems[J]. IEEE Access, 2020, 8: 47888-47899.
[16] Yu Y, Chen H, Chen L, et al. Optimal operation of the combined heat and power system equipped with power‐to‐heat devices for the improvement of wind energy utilization[J]. Energy Science & Engineering, 2019, 7(5): 1605-1620.
[17] Yifan Z, Wei H, Le Z, et al. Power and energy flexibility of district heating system and its application in wide-area power and heat dispatch[J]. Energy, 2020, 190: 116426.
[18] Zhou H, Li Z, Zheng J H, et al. Robust Scheduling of Integrated Electricity and Heating System Hedging Heating Network Uncertainties[J]. IEEE Transactions on Smart Grid, 2019, 11(2): 1543-1555.
[19] Turk A, Wu Q, Zhang M, et al. Day-ahead stochastic scheduling of integrated multi-energy system for flexibility synergy and uncertainty balancing[J]. Energy, 2020, 196: 117130.
[20] Eladl A A, El-Afifi M I, Saeed M A, et al. Optimal operation of energy hubs integrated with renewable energy sources and storage devices considering CO2 emissions[J]. International Journal of Electrical Power & Energy Systems, 2020, 117: 105719.
[21] Yi Z, Xu Y, Hu J, et al. Distributed, Neurodynamic-Based Approach for Economic Dispatch in an Integrated Energy System[J]. IEEE Transactions on Industrial Informatics, 2019, 16(4): 2245-2257.
[22] He L, Lu Z, Geng L, et al. Environmental economic dispatch of integrated regional energy system considering integrated demand response[J]. International Journal of Electrical Power & Energy Systems, 2020, 116: 105525.
[23] Li Y, Miao S, Yin B, et al. Combined heat and power dispatch considering advanced adiabatic compressed air energy storage for wind power accommodation[J]. Energy Conversion and Management, 2019, 200: 112091.
[24] Liu Y, Ye Y, Chen X, et al. Robust Day-Ahead Dispatch for Integrated Power-Heat-Gas Microgrid considering Wind Power Uncertainty[J]. Mathematical Problems in Engineering, 2020, 2020.
[25] Wang Y, Wang Y, Huang Y, et al. Operation optimization of regional integrated energy system based on the modeling of electricity-thermal-natural gas network[J]. Applied Energy, 2019, 251: 113410.
[26] Anand H, Narang N, Dhillon J S. Unit commitment considering dual-mode combined heat and power generating units using integrated optimization technique[J]. Energy Conversion and Management, 2018, 171: 984-1001.
[27] Santos M I, Uturbey W. A practical model for energy dispatch in cogeneration plants[J]. Energy, 2018, 151: 144-159.
[28] Rist J F, Dias M F, Palman M, et al. Economic dispatch of a single micro-gas turbine under CHP operation[J]. Applied Energy, 2017, 200: 1-18.
[29] Gu W, Wang J, Lu S, et al. Optimal operation for integrated energy system considering thermal inertia of district heating network and buildings[J]. Applied energy, 2017, 199: 234-246.
[30] Chen X, Wang C, Wu Q, et al. Optimal operation of integrated energy system considering dynamic heat-gas characteristics and uncertain wind power[J]. Energy, 2020: 117270.
[31] Li Z, Wang C, Li B, et al. Probability-Interval-Based Optimal Planning of Integrated Energy System With Uncertain Wind Power[J]. IEEE Transactions on Industry Applications, 2019, 56(1): 4-13.

[32] Lu S, Gu W, Zhou S, et al. Adaptive Robust Dispatch of Integrated Energy System Considering Uncertainties of Electricity and Outdoor Temperature[J]. IEEE Transactions on Industrial Informatics, 2019, 16(7): 4691-4702.
[33] Mohammadi H, Mohammadi M. Optimization of the micro combined heat and power systems considering objective functions, components and operation strategies by an integrated approach[J]. Energy Conversion and Management, 2020, 208: 112610.
[34] Zhang T, Yang C, Chen H, et al. Multi-objective optimization operation of the green energy island based on Hammersley sequence sampling[J]. Energy Conversion and Management, 2020, 204: 112316.
[35] Nazari-Heris F, Mohammadi-Ivatloo B, Nazarpour D. Economic Dispatch of Renewable Energy and CHP-Based Multi-zone Microgrids Under Limitations of Electrical Network[J]. Iranian Journal of Science and Technology, Transactions of Electrical Engineering, 2020, 44(1): 155-168.
[36] Mei J, Wang X, Kirtley J L. Optimal scheduling of real multi-carrier energy storage system with hydrogen-based vehicle applications[J]. IET Renewable Power Generation, 2019, 14(3): 381-388.
[37] Rigo-Mariani R, Zhang C, Romagnoli A, et al. A combined cycle gas turbine model for heat and power dispatch subject to grid constraints[J]. IEEE Transactions on Sustainable Energy, 2019, 11(1): 448-456.
[38] Jiang T, Min Y, Zhou G, et al. Hierarchical dispatch method for integrated heat and power systems considering the heat transfer process[J]. Renewable and Sustainable Energy Reviews, 135: 110412.
[39] Zheng J, Zhou Z, Zhao J, et al. Integrated heat and power dispatch truly utilizing thermal inertia of district heating network for wind power integration[J]. Applied energy, 2018, 211: 865-874.
[40] Zheng J, Zhou Z, Zhao J, et al. Effects of the operation regulation modes of district heating system on an integrated heat and power dispatch system for wind power integration[J]. Applied Energy, 2018, 230: 1126-1139.
[41] Wang W, Jing S, Sun Y, et al. Combined heat and power control considering thermal inertia of district heating network for flexible electric power regulation[J]. Energy, 2019, 169: 988-999.
[42] Alobaid F, Starkloff R, Pfeiffer S, et al. A comparative study of different dynamic process simulation codes for combined cycle power plants–Part A: Part loads and off-design operation[J]. Fuel, 2015, 153: 692-706.
[43] Shin J Y, Jeon Y J, Maeng D J, et al. Analysis of the dynamic characteristics of a combined-cycle power plant[J]. Energy, 2002, 27(12): 1085-1098.
[44] Montañés R M, GarÐarsdóttir S Ó, Normann F, et al. Demonstrating load-change transient performance of a commercial-scale natural gas combined cycle power plant with post-combustion CO2 capture[J]. International Journal of Greenhouse Gas Control, 2017, 63: 158-174.
[45] Mertens N, Alobaid F, Lanz T, et al. Dynamic simulation of a triple-pressure combined-cycle plant: Hot start-up and shutdown[J]. Fuel, 2016, 167: 135-148.
[46] Rua Pazos J. Dynamic Modeling and Process Simulation of Steam Bottoming Cycle[D]. NTNU, 2017.
[47] Alobaid F, Karner K, Belz J, et al. Numerical and experimental study of a heat recovery steam generator during start-up procedure[J]. Energy, 2014, 64: 1057-1070.
[48] Benato A, Stoppato A, Mirandola A. Dynamic behaviour analysis of a three pressure level heat recovery steam generator during transient operation[J]. Energy, 2015, 90: 1595-1605.

[49] Sunil P U, Barve J, Nataraj P S V. Mathematical modeling, simulation and validation of a boiler drum: Some investigations[J]. Energy, 2017, 126: 312-325.
[50] Benato A, Bracco S, Stoppato A, et al. Dynamic simulation of combined cycle power plant cycling in the electricity market[J]. Energy Conversion and Management, 2016, 107: 76-85.
[51] Yu H, Nord L O, Yu C, et al. An improved combined heat and power economic dispatch model for natural gas combined cycle power plants[J]. Applied Thermal Engineering, 2020, 181: 115939.
[52] Liu B, Wang L, Jin Y H, et al. Improved particle swarm optimization combined with chaos[J]. Chaos, Solitons & Fractals, 2005, 25(5): 1261-1271.
[53] Wan Z, Wang G, Sun B. A hybrid intelligent algorithm by combining particle swarm optimization with chaos searching technique for solving nonlinear bilevel programming problems[J]. Swarm and Evolutionary Computation, 2013, 8: 26-32.
[54] Alatas B, Akin E, Ozer A B. Chaos embedded particle swarm optimization algorithms[J]. Chaos, Solitons & Fractals, 2009, 40(4): 1715-1734.
[55] Gandomi A H, Yun G J, Yang X S, et al. Chaos-enhanced accelerated particle swarm optimization[J]. Communications in Nonlinear Science and Numerical Simulation, 2013, 18(2): 327-340.
[56] Cai J, Ma X, Li L, et al. Chaotic particle swarm optimization for economic dispatch considering the generator constraints[J]. Energy conversion and management, 2007, 48(2): 645-653.
[57] Ringkjøb H K, Haugan P M, Solbrekke I M. A review of modelling tools for energy and electricity systems with large shares of variable renewables[J]. Renewable and Sustainable Energy Reviews, 2018, 96: 440-459.
[58] Guo S, Liu Q, Sun J, et al. A review on the utilization of hybrid renewable energy[J]. Renewable and Sustainable Energy Reviews, 2018, 91: 1121-1147.
[59] Musa S D, Zhonghua T, Ibrahim A O, et al. China's energy status: A critical look at fossils and renewable options[J]. Renewable and Sustainable Energy Reviews, 2018, 81: 2281-2290.
[60] Das H S, Rahman M M, Li S, et al. Electric vehicles standards, charging infrastructure, and impact on grid integration: A technological review[J]. Renewable and Sustainable Energy Reviews, 2020, 120: 109618.
[61] Zhou Y, Cao S, Hensen J L M, et al. Energy integration and interaction between buildings and vehicles: A state-of-the-art review[J]. Renewable and Sustainable Energy Reviews, 2019, 114: 109337.
[62] Mahmud K, Town G E, Morsalin S, et al. Integration of electric vehicles and management in the internet of energy[J]. Renewable and Sustainable Energy Reviews, 2018, 82: 4179-4203.
[63] Zheng Y, Niu S, Shang Y, et al. Integrating plug-in electric vehicles into power grids: A comprehensive review on power interaction mode, scheduling methodology and mathematical foundation[J]. Renewable and Sustainable Energy Reviews, 2019, 112: 424-439.
[64] Pomianowski M Z, Johra H, Marszal-Pomianowska A, et al. Sustainable and energy-efficient domestic hot water systems: A review[J]. Renewable and Sustainable Energy Reviews, 2020, 128: 109900.
[65] Fischer D, Madani H. On heat pumps in smart grids: A review[J]. Renewable and Sustainable Energy Reviews, 2017, 70: 342-357.